International Journal of Current Trends in Engineering & Technology
ISSN: 2395-3152
Volume: 09, Issue: 06 (November-December, 2023)

Exploration and Categorization of Electrocardiogram Signals through the Application of Edge Computing

Chandra Prakash [1], Sarwesh Site [2]
[1,2] Department of Computer Science and Engineering
All Saints' College of Technology, Bhopal, India

Abstract

This article presents a comprehensive analysis and categorization of Electrocardiogram (ECG) signals, leveraging the power of edge computing. The study focuses on enhancing the performance of a 12-channel ECG arrhythmia categorization system by implementing advanced oversampling and undersampling techniques. Notably, Random Oversampling (ROS) emerges as particularly effective, demonstrating significant improvements over models trained with original data. Despite commendable performance across various cases, ROS stands out for its straightforward implementation, making it a preferred choice for robust ECG signal categorization. The findings contribute to the refinement of ECG signal processing methodologies, especially in the context of edge computing applications.
Keywords: Electrocardiogram (ECG), Signal Analysis, Edge Computing, Machine Learning, Deep Learning

1 Introduction

The development of sophisticated health monitoring systems has consistently been a subject of active investigation. Over the past few decades, a multitude of portable devices have been introduced to facilitate early detection and diagnosis of heart failure, a prevalent, expensive, debilitating, and potentially fatal syndrome. These advanced heart-monitoring devices exhibit the capability to deliver dependable and precise heart monitoring, identifying sporadic events during periods of ambiguity. Operating akin to a black box, these devices possess the potential to improve decision-making processes by alerting healthcare professionals to the necessity of patient readmission, thereby serving as an effective alternative with the potential to save lives [1].

Research in artificial intelligence (AI), particularly advancements in machine learning (ML) and deep learning (DL), has resulted in groundbreaking innovations across various domains, including radiology, pathology, and genomics. Modern DL models, characterized by millions of parameters, require learning from extensive, curated datasets to achieve clinical-grade accuracy. This learning process is essential for ensuring safety, fairness, equity, and robust generalization to unseen data [2].

In conventional centralized machine learning (ML) approaches, data storage and model training typically occur on high-performance cloud servers. Multiple edge nodes collaborate with the remote cloud to execute large distributed tasks, involving both local processing and remote coordination. The traditional cloud computing model is not well-suited for applications requiring low latency, leading to the emergence of a new computational paradigm known as edge computing. Edge computing focuses on facilitating data transmission among devices at the edge, closer to user applications, rather than relying on a centralized server. The edge node, usually a resource-constrained device used by the end user, is geographically close to the nearest edge server, which possesses ample computing resources and high bandwidth for communication with end nodes. When additional computing power is needed, the edge server connects to the cloud server [3].

2 The ECG Waveform

During the ECG recording, voltage-versus-time signals are generated, typically presented in millivolts (mV) versus seconds. Figure 1 illustrates a typical Lead II ECG waveform. In this Lead II recording, the negative electrode was positioned on the right wrist and the positive electrode on the left ankle. Consequently, a sequence of peaks and waves is evident, each corresponding to ventricular or atrial depolarization and repolarization, with each segment of the signal indicating a distinct event in the cardiac cycle.

The ECG captures three primary waveforms.(1):

- The P-wave
- QRS complex
- T-wave.

The ECG records three primary waveforms: the P-wave, generated by atrial depolarization; the QRS complex, resulting from ventricular depolarization; and the T-wave, associated with ventricular repolarization. These waveforms typically follow a recurring rhythm known as sinus rhythm, originating from the sinoatrial (SA) node.

International Journal of Current Trends in Engineering & Technology
ISSN: 2395-3152
Volume: 09, Issue: 06 (November-December, 2023)

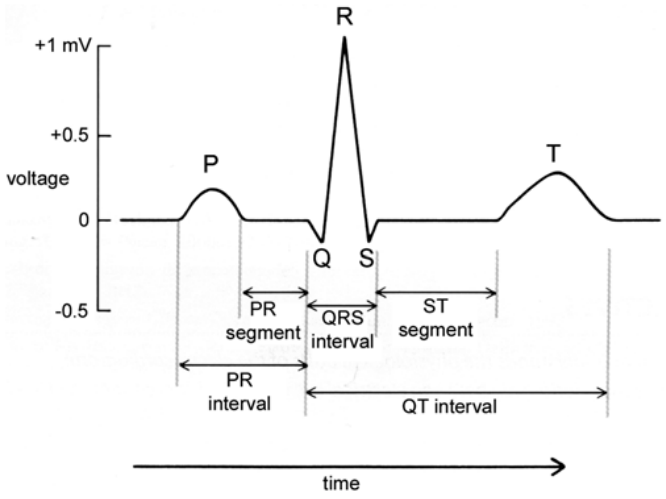

Figure 1: A typical ECG waveform for one cardiac cycle, measured from the Lead II position [4].

Occasionally, a fourth waveform called a U-wave may be observed, particularly at slower heart rates, although its significance remains uncertain. Some researchers propose that it signifies the later stages of ventricular repolarization, while others describe it as a post-repolarization phenomenon. U-wave abnormalities have been noted in various disease states, including ischemic heart disease [5].

The cardiac cycle begins with the depolarization of the sinoatrial (SA) node located in the right atrium. Although a conventional ECG cannot detect this early firing due to the insufficient number of cells in the node providing a measurable electrical potential, the right and left ventricles continue to depolarize following the P-wave. This results in the observable QRS complex, lasting approximately 100 milliseconds, where the Q-wave is the initial negative deflection (if present), the R-wave is the largest positive deflection, and the S-wave is the smallest positive deflection [6].

The T-wave typically marks the conclusion of a cardiac cycle, followed by the P-wave of the subsequent cycle, and so forth. As ventricular contraction concludes, the ECG signal returns to baseline, and the ventricles undergo repolarization. Atrial contractions cease, and atrial repolarization coincides with the QRS complex, although it is not usually detectable in an ECG due to its overshadowing by the much larger tissue volume involved in ventricular depolarization [4].

3 The 12-leads ECG

An ECG lead serves as a representation of the heart's electrical activity observed from a specific perspective. Therefore, when conducting a 12-lead ECG, the recording captures cardiac electrical activity from 12 different viewpoints [6]. To illustrate, consider visiting a historical structure and capturing images of it. If you take 12 photos from diverse angles around the structure, each image will reveal distinct aspects, such as the front, sides, and back. These images collectively form a three-dimensional record, portraying the structure's shape and appearance comprehensively. In a similar fashion, a 12-lead ECG generates a three-dimensional representation of the heart's electrical activity.

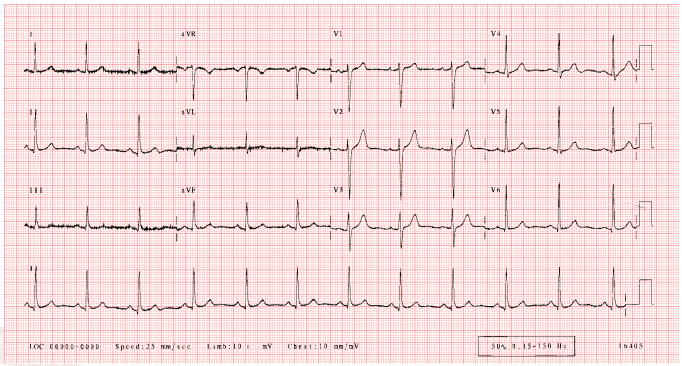

Figure 2: 12-leads normal ECG

The recording of multiple images depicting the heart's electrical activity depends on the type of machine employed and the number of electrodes used. The use of 12-lead ECG devices is prevalent among healthcare professionals, where 12 distinct electrical images of the heart are measured and recorded (Figure 2). In essence, a 12-lead ECG captures the electrical activity of the heart from 12 different perspectives. For instance, Lead II monitors electrical activity from the heart's inferior (diaphragmatic) surface and is frequently employed to measure heart rate [7].

4 Arrhythmia Types

Analyzing arrhythmias proves challenging because each individual possesses a unique ECG, varying from one person to another and even changing dramatically within a short timeframe. Mere memorization of common ECG patterns for future recognition is insufficient. Identifying patterns is a prevalent yet unintentional approach to arrhythmia analysis via ECG ([8]). Arrhythmias are broadly categorized into two types:

1. **Rhythmic**: Characterized by a sequence of irregular beats.

2. **Morphological**: Comprising abnormal single beats.

This article primarily focuses on the classification of the first type of arrhythmias, with categorization provided by SNOMED CT. SNOMED CT is a globally accepted terminology package, offering a comprehensive and precise language for clinical IT systems, facilitating easier, safer, and more accurate data exchange. It covers a wide range, including processes, symptoms, clinical measurements, diagnoses, and drugs.

For the Physionet 2020 challenge, around 27 of the most frequently encountered arrhythmias were considered. However, the following paragraphs provide in-depth explanations of all potential arrhythmias. The complete list of categories can be found in the GitHub repository cited in [9].

5 Related Work

Seeuws *et al.* [10] examined the application of auto-encoders, a subset of unsupervised deep learning models, for assessing the quality of ECG signals. Two quality indicators derived from a trained auto-encoder, namely AE-logMSE and AE-LLH, consistently exhibited strong performance across the evaluated tasks in comparison to established benchmarks. The evaluation tasks extended beyond the conventional anomaly detection scenarios for auto-encoders. In addition to excelling in binary quality scoring, AE-logMSE and AE-LLH demonstrated robust performance in assessing correlation with various noise levels.

Hinatsu et al. explored the estimation of cardiovascular signals, specifically electrocardiogram (ECG) and photoplethysmogram (PPG) waveforms, by utilizing skin vibrations in the form of piezoelectric plethysmogram (PEPG) signals. ECG and PPG measurements hold significance in biomedical and security applications, and PEPG signals offer a means to estimate ECG and PPG waveforms based on physiological activities in the cardiovascular system. The research delved into the estimation procedure for ECG and PPG signal waveforms from PEPG signals employing frequency analysis. An experiment was conducted using a dataset that included ECG, PPG, and PEPG signals to assess estimation performance. The outcomes reveal successful estimation of ECG and PPG waveforms from PEPG signals, with errors of less than 15% and 10%, respectively.

Edla *et al.* [11] formulated statistical techniques to dynamically model and estimate parameters of ECG signals utilizing sequential Bayesian approaches. They implemented a straightforward Bayesian Maximum Likelihood (ML) classifier to differentiate between various cardiac conditions. These models offer the benefit of eliminating the need for user-defined parameters, conducting early-stage processing to acquire a priori information about ECG signals for filter initialization or ECG fiducial point delineation, and adapting to alterations in ECG signal morphology. The derived model parameters furnish features suitable for the automatic classification of cardiac arrhythmias, diminishing the reliance on manual annotation and facilitating prompt diagnoses.

Lee *et al.* [12] utilized a Generative Adversarial Network (GAN) to produce V-leads ECG signals derived from MLII lead ECG signals, specifically a limb lead. This study distinguishes itself from prior research by incorporating R-peak alignment, ordered time-sequence embedding, and the use of a paired dataset. Unlike current portable ECG devices, which often provide limited ECG signals from limb leads, this study addresses the limitations by introducing methods like R-peak detection and S-T segment analysis for ECG applications. The accuracy of ECG pattern reconstruction is deemed crucial for the efficacy of these applications. The R-peak-aligned GAN explored in this study has the potential to enable the retrieval of lead-ECG signals via portable ECG leads, making the recovered data applicable in both mobile environments and clinical settings. Additionally, the one-to-multi lead reconstruction may contribute to the advancement of sophisticated portable ECG hardware, alleviating issues related to the inconvenience of attaching multiple leads and data storage space limitations.

Tobón and Falk [13] introduced a novel approach to enhance the denoising of ECG signals through spectro-temporal filtering. Comparative assessments with a state-of-the-art wavelet-based enhancement algorithm demonstrated the superiority of the proposed method across various performance metrics, particularly in extremely noisy conditions. Specifically, the suggested method exhibited an approximately 11 dB improvement in Signal-to-Noise Ratio (SNR) and achieved a Heart Rate (HR) error percentage of 2%, as opposed to 57% in the presence of the noisy signal and 6% with the wavelet-enhanced ECG. The proposed solution not only elevated SNR and HR estimation but also enhanced heart rate variability measurement, presenting opportunities for accurate ECG data analysis with low-cost devices in field settings. However, further investigation is essential to validate these findings in a controlled clinical environment, involving scenarios like abrupt changes in heart rate, such as arrhythmia, especially in conditions like atrial fibrillation or significant ventricular entropy.

6 Proposed Method

The proposed approach for predicting ECG diagnoses involves the use of a Deep Neural Network (DNN). A DNN is a collection of algorithms designed to recognize patterns in a dataset by emulating the functioning of the human brain.

In this context, deep neural networks refer to systems of neurons, whether organic or artificial ([14]). Deep neural networks exhibit the ability to adapt to changing inputs,

providing optimal results without the need to modify output criteria. Neural networks, rooted in artificial intelligence, are rapidly gaining prominence in the development of trading systems.

Neural networks find applications in various financial tasks, including time-series forecasting, algorithmic trading, securities classification, credit risk modeling, and the generation of proprietary indicators and price derivatives in the financial domain ([15] [16]). The structure of a deep neural network is analogous to that of the human brain's neural network. In the context of a deep neural network, a "neuron" is a mathematical function that gathers and categorizes data based on a set of rules, closely resembling the principles of curve fitting and regression analysis, two statistical methods.

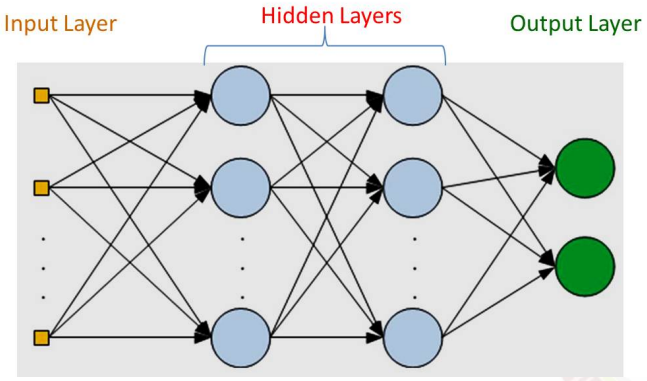

Figure 3: Deep Neural Network (Multi-layer Perceptron) schema

In a multi-layered perceptron (MLP), perceptrons are organized into interconnected layers, as illustrated in Figure 3 [16]. The input layer is responsible for gathering input patterns, while the output layer maps input patterns to classifications or output signals. Hidden layers play a crucial role in refining the input weightings until the neural network achieves minimal error margin. The purpose of hidden layers is to deduce significant elements from input data that can predict outcomes, resembling the concept of feature extraction. This process is analogous to how statistical methods like principal component analysis operate ([16])

7 Result Analysis

A confusion matrix, as depicted in Table 1, illustrates the performance of a classification model on test data where the true values are known ([17]). While the confusion matrix is straightforward, the associated terminology can be perplexing. In the examples below, A hypothetical target variable is introduced named "Diagnose A" with values "Yes" (indicating the recording belongs to that diagnosis) and "No" (indicating the recording does not belong to that diagnosis).

Here is an elucidation for each of the elements in the matrix to comprehend the terminology mentioned earlier ([17] [18]).

- *True negatives (TN):* The model correctly predicted the absence of diagnosis A, and indeed, there is no diagnosis A.
- *True positives (TP):* These instances are where the model predicted yes (the recording has diagnosis A), but it doesn't.
- *False positives (FP):* The model forecasted that there would be diagnosis A, but it is not present. (This is also known as a "Type I error.")
- *False negatives (FN):* The model expected that there would be no diagnosis A, yet it is present. (This is often termed a "Type II error.")

7.0.1 Accuracy

$$\text{Accuracy} = \frac{\text{TP} + \text{TN}}{\text{TP} + \text{FP} + \text{FN} + \text{TN}} \tag{1}$$

The most fundamental performance metric is accuracy, representing the ratio of correctly predicted observations to all observations. Accuracy is considered a relevant measure when datasets are symmetric, and the number of false positives and false negatives is roughly equal.

Consider a scenario where the training set comprises 98

The real challenge arises when the cost of misclassifying minority class samples becomes significant. In situations where the cost of failing to diagnose a serious illness is much higher than the cost of subjecting a healthy person to additional tests, dealing with rare but life-threatening disorders, accuracy alone may not provide an accurate evaluation ([18]).

7.0.2 Precision

$$\text{Precision} = \frac{\text{TP}}{\text{TP} + \text{FP}} \tag{2}$$

Precision ([17]) is the ratio of correctly predicted positive observations to the total expected positive observations. It addresses the question of how many of the identified positive instances were accurate. Precision is particularly relevant when aiming for a low false-positive rate.

Precision serves as a valuable metric when the costs associated with false positives are substantial. For instance, in email spam detection, a false positive occurs when an email that is not spam (actual negative) is incorrectly identified as spam (predicted spam). A low precision in the spam detection model may lead to the user missing important emails.

Table 1: Confusion Matrix representation

	Actual Class	
Predicted Class	Diagnose A - YES = 1	Diagnose A - NO = 0
Diagnose A - YES = 1	True Positives (**TP**)	False Positives (**FP**)
Diagnose A - NO = 0	False Negatives (**FN**)	True Negatives (**TN**)

7.0.3 Recall

$$\text{Recall} = \frac{\text{TP}}{\text{TP} + \text{FN}} \tag{3}$$

Recall ([17]) is the ratio of correctly predicted positive observations to all observations in the actual class. It addresses the question of how many instances of the actual positive class were accurately identified.

In scenarios such as identifying sick patients, a false negative occurs when a sick patient (actual positive) undergoes a test and is predicted to be healthy (predicted negative). In situations where the condition is infectious, the cost associated with a false negative is likely to be significant.

7.0.4 F1 Score

$$\text{F1 Score} = \frac{2 \times (\text{Recall} \times \text{Precision})}{(\text{Recall} + \text{Precision})} \tag{4}$$

The F1-Score is the weighted average of Precision and Recall, taking into account both false positives and false negatives in the score. Despite being less intuitive than accuracy, F1 is often more valuable, especially when dealing with unequal class distributions and varying costs of false positives and false negatives ([18] [17]). While accuracy works well when the costs of false positives and false negatives are equal, Precision and Recall are crucial metrics when the costs differ significantly.

8 Conclusion and Future Work

In this research, the DNN trained with ROS data emerged as the best model, exhibiting an Overall Index of 0.55 and an F1-Score of 0.55. However, when incorporating more than four local nodes, utilizing proposed approach with oversampled data yielded more consistent results. Therefore, proposed method is recommended for implementation in scenarios with a large number of nodes. Conversely, DNN with ROS data is the preferred choice for situations involving a small number of clients.

References

[1] A. Scirè, F. Tropeano, A. Anagnostopoulos, and I. Chatzigiannakis, "Fog-computing-based heartbeat detection and arrhythmia classification using machine learning," *Algorithms*, vol. 12, no. 2, 2019. [doi: https://www.mdpi.com/1999-4893/12/2/32

[2] N. Rieke, J. Hancox, W. Li, F. Milletarì, H. R. Roth, S. Albarqouni, S. Bakas, M. N. Galtier, B. A. Landman, K. Maier-Hein, S. Ourselin, M. Sheller, R. M. Summers, A. Trask, D. Xu, M. Baust, and M. J. Cardoso, "The future of digital health with federated learning," *npj Digital Medicine*, vol. 3, no. 1, sep 2020. [doi: https://doi.org/10.1038%2Fs41746-020-00323-1

[3] Q. Xia, W. Ye, Z. Tao, J. Wu, and Q. Li, "A survey of federated learning for edge computing: Research problems and solutions," *High-Confidence Computing*, vol. 1, no. 1, p. 100008, 2021. [doi: https://www.sciencedirect.com/science/article/pii/S266729522100009X

[4] P. Iaizzo, *Handbook of cardiac anatomy, physiology, and devices, third edition.* Springer International Publishing, Jan. 2015.

[5] M. Sampson and A. Mcgrath, "Understanding the ecg. part 1: Anatomy and physiology," *British Journal of Cardiac Nursing*, vol. 10, pp. 548–554, 11 2015.

[6] ——, "Understanding the ecg part 2: Ecg basics," *British Journal of Cardiac Nursing*, vol. 10, pp. 588–594, 12 2015.

[7] G. Walraven, *Basic Arrhythmias.* Pearson Education, 2014. [doi: https://books.google.ne/books?id=5f67AQAAQBAJ

[8] S. Goldsworthy, R. Kleinpell, and G. Williams, *International Best Practices in Critical Care.* New York, NY :: World Federation of Critical Care Nurses,, 2017.

[9] E. Perez and matthewreyna, "physionetchallenges," 03 2021. [doi: https://github.com/physionetchallenges/physionetchallenges.github.io/blob/master/2020/Dx_map.csv

[10] N. Seeuws, M. De Vos, and A. Bertrand, "Electrocardiogram quality assessment using unsupervised deep learning," *IEEE Transactions on Biomedical Engineering*, vol. 69, no. 2, pp. 882–893, 2022. [doi: https://doi.org/10.1109/TBME.2021.3108621

[11] S. Edla, N. Kovvali, and A. Papandreou-Suppappola, "Electrocardiogram signal modeling with adaptive parameter estimation using sequential bayesian methods," *IEEE Transactions on Signal Processing*, vol. 62, no. 10, pp. 2667–2680, 2014. [doi: https://doi.org/10.1109/TSP.2014.2312316

[12] J. Lee, K. Oh, B. Kim, and S. K. Yoo, "Synthesis of electrocardiogram v-lead signals from limb-lead

measurement using r-peak aligned generative adversarial network," *IEEE Journal of Biomedical and Health Informatics*, vol. 24, no. 5, pp. 1265–1275, 2020. [doi: https://doi.org/10.1109/JBHI.2019.2936583

[13] D. P. Tobón and T. H. Falk, "Adaptive spectro-temporal filtering for electrocardiogram signal enhancement," *IEEE Journal of Biomedical and Health Informatics*, vol. 22, no. 2, pp. 421–428, 2018. [doi: https://doi.org/10.1109/JBHI.2016.2638120

[14] I. Basheer and M. Hajmeer, "Artificial neural networks: Fundamentals, computing, design, and application," *Journal of microbiological methods*, vol. 43, pp. 3–31, 01 2001.

[15] C. Gallo, *Artificial Neural Networks: tutorial*, 01 2015.

[16] M.-C. Popescu, V. Balas, L. Perescu-Popescu, and N. Mastorakis, "Multilayer perceptron and neural networks," *WSEAS Transactions on Circuits and Systems*, vol. 8, 07 2009.

[17] G. Canbek, S. Sagiroglu, T. Taskaya Temizel, and N. Baykal, "Binary classification performance measures/metrics: A comprehensive visualized roadmap to gain new insights," 10 2017, pp. 821–826.

[18] M. Hossin and S. M.N, "A review on evaluation metrics for data classification evaluations," *International Journal of Data Mining and Knowledge Management Process*, vol. 5, pp. 01–11, 03 2015.